Journal of Thermal Analysis and Calorimetry, Vol. 96 (2009) 2, 575–582

THERMAL STUDY OF AN EPOXY SYSTEM DGEBA (*n*=0)/MXDA MODIFIED WITH POSS

M. Villanueva[*], *J. L. Martín-Iglesias, J. A. Rodríguez-Añón and J. Proupín-Castiñeiras*

Research Group TERBIPROMAT, Departamento de Física Aplicada, Universidade de Santiago de Compostela, Campus Sur, 15782 Santiago de Compostela, Spain

The thermal degradation of the epoxy system diglycidyl ether of bisphenol A (DGEBA *n*=0) and *m*-xylylenediamine (*m*XDA) containing different concentrations of polyhedral oligomeric silsesquioxanes (POSS) nanoparticles was studied by thermogravimetric analysis in order to determine the influence of both, the POSS concentration and the curing cycle on the degradation process and to compare it with the results for the non modified system.

Glass transition temperatures for the same systems were also determined by differential scanning calorimetry. Different behaviors have been observed, depending on the POSS concentration and on the curing selection.

Keywords: *activation energy, DSC, epoxy resin, glass transition temperature, polyhedral oligomeric silsesquioxanes nanoparticles, TG*

Introduction

Polymers have a great interest for the study and design of new materials. Among these materials are epoxy resins, which have good properties, such as low shrinkage during cure, good adhesion, high water and chemical resistance, etc. They have also fast and easy cure in a broad range of temperatures. For many end-uses, it is necessary to add other components to the resin in order to improve its properties. Recently, macromolecules containing polyhedral oligomeric silsesquioxanes (POSS) nanoparticles have been considered for many researchers to be added to this kind of systems due to efficiency in the design of hybrid materials [1]. This type of nanoparticles has a chemical structure (RSiO1.5)n, where *R* may be a wide variety of functional groups [2–7]. In this work, octameric polyhedral silsesquioxanes have been employed. They have a SiO cage structure very similar to that of silica particles with eight vertices. Each vertex may be functionalized for specific applications. The incorporation of POSS reagents that contain reactive groups into organic polymer systems creates the possibility of nanoscale reinforcement with POSS bound to the polymer chain with chemical bonds [2].

POSS reagents combine a hybrid inorganic-organic composition with nanosized cage structures having dimensions comparable to those of most polymeric segments or coils [8].

Hence incorporation of POSS reagents into linear thermoplastics or thermoset networks can be used to modify the composition, local structure and chain mobility in polymeric systems. These modifications can ultimately affect the thermal, oxidative and dimensional stability of many polymeric resins, thus upgrading their properties for numerous high-performance engineering applications [1, 2].

Since the behavior of thermosets can be affected by the addition of nanoparticles, it is interesting to investigate the changes that take place during the thermal degradation of these materials. The study of the degradation of a polymer is important because it can determine the upper temperature limit, the mechanism of a solid-state process and the life-time for a thermoset. Many studies are focused on the thermal degradation of this kind of materials [9] although the knowledge of the kinetics of the curing reaction is also interesting to predict some final properties [10].

The main objective of this work was to study the influence of the addition of different concentrations of POSS nanoparticles on the thermal properties of an epoxy-diamine system obtained through two different curing cycles. Properties such as glass transition temperature and main decomposition temperature were determined. The kinetics of thermal degradation in non-isothermal conditions was also studied.

Kinetic methods

TG non-isothermal experiments register the change of the sample mass as a function of temperature. Kinetic parameters can be extracted from non-isothermal

* Author for correspondence: maria.villanueva@usc.es

1388–6150/$20.00

Akadémiai Kiadó, Budapest, Hungary
Springer, Dordrecht, The Netherlands

experiments. The degree of conversion can be expressed as:

$$\alpha = \frac{m_0 - m}{m_0 - m_\infty} \quad (1)$$

where m is the measured experimental mass at temperature T, m_0 the initial mass and m_∞ the mass at the end of non-isothermal experiments. The rate of conversion, $d\alpha/dt$ is a linear function of a temperature-dependent rate constant, k and a temperature-independent function of conversion, α, that is:

$$\frac{d\alpha}{dt} = kf(\alpha) \quad (2)$$

Substituting Arrhenius equation into Eq. (2), one obtains:

$$\frac{d\alpha}{dt} = Af(\alpha)e^{-\frac{E}{RT}} \quad (3)$$

If the temperature of the sample is changed by a controlled and constant heating rate, $\beta = dT/dt$, the variation in the degree of conversion can be analyzed as a function of temperature, this temperature being dependent on the time of heating. Therefore, the reaction rate gives:

$$\frac{d\alpha}{dT} = \frac{A}{\beta}e^{-\frac{E}{RT}}f(\alpha) \quad (4)$$

Integration of this equation from an initial temperature, T_0, corresponding to a null degree of conversion, to the peak temperature of the derivative thermogravimetric curve (DTG), T_p, where $\alpha = \alpha_p$ gives [11]:

$$g(\alpha) = \int_0^{\alpha_p} \frac{d\alpha}{f(\alpha)} = \frac{A}{\beta}\int_0^{T_p} e^{-\frac{E}{RT}}dT \quad (5)$$

where $g(\alpha)$ is the integral function of conversion. In the case of polymers, this integral function, $g(\alpha)$, is either a sigmoidal function (A_2, A_3, A_4) or a deceleration function (R_n, n=1–3; D_n, n=1–4 and F_n, n=1–3). In the bibliography different expressions of $g(\alpha)$ for the different solid state mechanisms can be found [12–15]. These functions were satisfactorily employed for the estimation of the reaction solid state mechanism from non-isothermal TG experiments [16].

Some methods, called integral methods, involve an approximate integration of Eq. (5). Three different integral methods are discussed in the present paper: Coats–Redfern, Horowitz–Metzger and Van Krevelen methods.

Coats–Redfern method [17]

Coats–Redfern used an asymptotic approximation for resolution of Eq. (5) obtaining:

$$\ln\frac{g(\alpha)}{T^2} = \ln\frac{AR}{\beta E} - \frac{E}{RT} \quad (6)$$

Activation energy for each degradation process can be determined from a plot of $\ln g(\alpha)$ *vs*. 1000/T.

Van Krevelen *et al*. [18] and Horowitz and Metzger [19] methods

Van Krevelen *et al*. made the first serious theoretical treatment of thermogravimetric data. These authors approximated the exponential integral to obtain a final equation in logarithmic form:

$$\log g(\alpha) = \log B + \left(\frac{E}{RT_r} + 1\right)\log T \quad (7)$$

where

$$B = \frac{A}{\beta}\left(\frac{E}{RT_r} + 1\right)^{-1}\left(\frac{0.368}{T_r}\right)^{\frac{E}{RT_r}}$$

and T_r is a reference temperature. Activation energy for each degradation process can be determined from a plot of $\log g(\alpha)$ *vs*. $\log T$.

Horowitz and Metzger simplify the exponential integral using an approximation similar to Van Krevelen *et al*., defining a characteristic temperature θ such that $\theta = T - T_r$ where T_r is a reference temperature. Making the approximation

$$\frac{1}{T} = \frac{1}{T_r + \theta} \cong \frac{1}{T_r} - \frac{\theta}{T_r^2}$$

they finally obtain for n=1;

$$\ln g(\alpha) = \frac{E\theta}{RT_r^2} \quad (8)$$

In this method, activation energy can be determined from a plot of $\ln g(\alpha)$ *vs*. θ.

Both methods present the problem of the arbitrary selection of the reference temperature. In this study, in order to obtain reproducible results, the reference temperature was taken as that corresponding to the maximum temperature rate. In this article we followed Van Krevelen *et al*. and Horowitz and Metzger's suggestions when they say that the selection of this arbitrary temperature does not affect the integral approximation of the kinetic model. Using any of these two methods, the activation energy can be determined without the precise knowledge of the thermodegradation kinetics.

Experimental

Materials

The epoxy resin was a commercial diglycidyl ether of bisphenol A, DGEBA (*n*=0) (Resin 332, Sigma Chemical Co. San Louis, USA) with an equivalent molecular mass of 173.6 g eq^{-1}, as determined by wet analysis [20]. The curing agent was *meta*-xylylenediamine, mXDA (Aldrich) with 99% purity, with an amine hydrogen equivalent mass of 34 g. The employed POSS was POSS®-Epoxy-cyclohexyl-isobutyl substituted (Aldrich) with molecular weight 941.66, epoxy equivalent of the same value; powder.

Epoxy resin, curing agent and POSS as used for the different studied systems are shown in Fig. 1.

Sample preparation

The DGEBA monomer was first preheated at 40°C to ensure that no crystals were present. Powder POSS was also preheated at 70°C during 1 h. Then, the mass of POSS necessary for the preparation of the sample was mixed with tetrahydrofuran (THF) and stirred by hand until a homogeneous liquid was obtained. After this mixing, the corresponding mass of DGEBA was added to the liquid and stirred by hand again. After 24 h at ambient temperature and other 24 h at 40°C, the THF was completely evaporated. A stoichiometric amount of curing agent was incorporated to the sample and the full system was stirred by hand. Finally, the sample was introduced in a cylindrical frame.

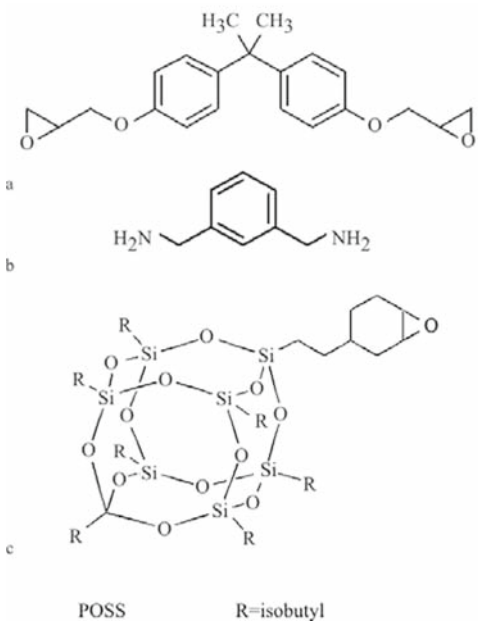

Fig. 1 Chemical structures a – Epoxy Resin: diglycidyl ether of bisphenol A (*n*=0), DGEBA, b – Hardener: *m*-xylylenediamine, mXDA, c – POSS®-Epoxy-cyclohexyl-isobutyl substituted, POSS

Amounts of POSS between 3 and 20% of the DGEBA mass were employed.

Two curing sequences were programmed according to a TTT diagram calculated for the system DGEBA/mXDA [20]:

- 'Short' or reference curing cycle (A systems), that consisted of two stages: a first step 20 min at 40°C and a second one 3 h at 105°C.
- 'Long' curing cycle (B systems) consisting of two isothermal steps: a first step 2 h at 70°C and a second one 7.5 h at 120°C.

After curing, the samples were removed from the frame and kept in a dry place at ambient temperature until use.

Methods

For thermogravimetric analysis, samples were cut, keeping similar geometry, in the form of 16–18 mg in mass. Thermogravimetric analysis was performed using a thermogravimetric analyzer (TGA7) from Perkin Elmer controlled by a PC. This microbalance was calibrated making use of the discontinuous change in the magnetic properties of perkalloy and alumel on heating. The Curie point of every metal was calculated by the microbalance, which was calibrated at different heating rates. The system was operated in the dynamic mode in the temperature range 100–800°C, at heating rate 20°C min^{-1}. All the experiments were carried out under a dry nitrogen atmosphere.

For calorimetric analysis (DSC), samples of 10 mg in mass were used. A Perkin-Elmer DSC7 unit, under control of a 1020 system controller, was used for calorimetric measurements. The experiments were carried out in a temperature range from 5 to 250°C at a heating rate 10°C min^{-1}. Because of the low temperature values necessary for the performance of measurements, a cooling device (Intercooler II supplied by Perkin-Elmer) was adapted to DSC-7 equipment. Because of the wide temperature range used in this study, the calorimeter was calibrated using two standards (indium and bidistilled water obtained by the milipore method).

Results and discussion

Calorimetric analysis (DSC)

From a first dynamic scan at a heating rate of 10°C min^{-1} glass transition temperatures, T_g, for the different systems were obtained. These temperatures were determined according to the half-width criterion using the Pyris software supplied with the equipment. Second dynamic scans at the same heating rate were performed in order to study possible residual curing effects. Ob-

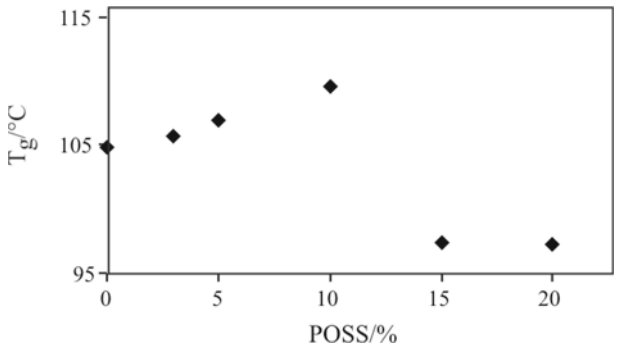

Fig. 2 Glass transition temperatures obtained from 1st DSC scans for samples cured through the short curing cycle

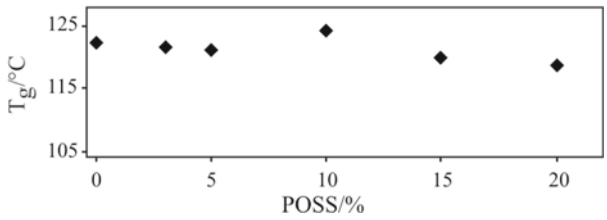

Fig. 3 Glass transition temperatures obtained from 2nd DSC scans for samples cured through the short curing cycle

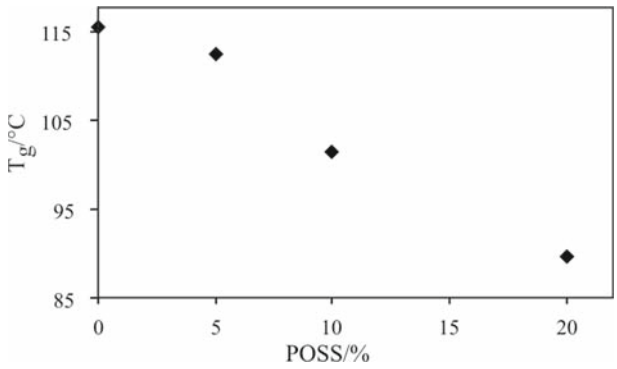

Fig. 4 Glass transition temperatures obtained from 1st DSC scans for samples cured through the long curing cycle

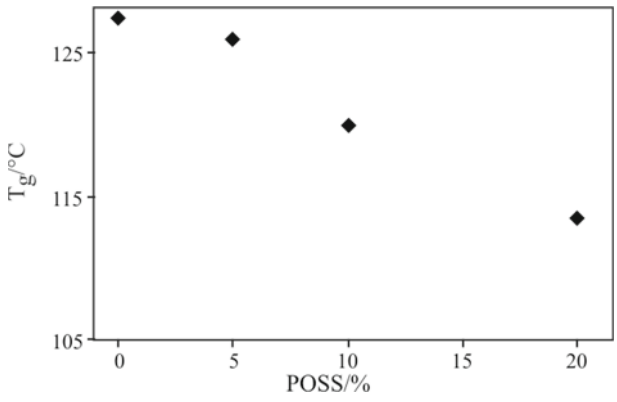

Fig. 5 Glass transition temperatures obtained from 2nd DSC scans for samples cured through the long curing cycle

tained results, corresponding to the two selected curing cycles (A and B systems), are shown in Figs 2–5.

Figure 2 shows the obtained results for the first scans corresponding to samples cured through the short curing cycle. As it can be seen, there is a linear increase in T_g with the POSS percentage for values below 10%. For higher POSS contents there is a significant and sharp decrease, even until lower values compared to those of the material without POSS. Therefore, we can conclude that, according to the T_g values, the optimum POSS percentage for this curing cycle could be around 10%. A future study should include percentages between 5 and 10% and 10 and 15% to better visualize the predicted decreasing behavior at intermediate percentages.

Figure 3 shows the obtained results for the second scans corresponding to the same samples cured through the short curing cycle. In this case, there is not a behavior as clear as that observed for the first scans. It can be noted that there is a T_g decrease with the POSS content, although there is a maximum for the sample containing 10% of POSS. It can also be mentioned that all obtained T_g values from these second scans were lower than $T_{g\infty}$ corresponding to the system without POSS [20], that was 126.10°C.

Figures 4 and 5 show the results corresponding to the samples cured through the long curing cycle, obtained for the first and second DSC scans, respectively. As it can be seen in Fig. 4, there is a decrease on T_g with the POSS content, although this behavior should be more defined with the study of more percentages. Anywhere, this tendency is different to that observed for A type samples. T_g values for the system without POSS are higher for the B type sample, as it should be expected for a higher extent of the curing reaction corresponding to a curing cycle developed at higher temperatures, but for the two highest POSS contents, T_g values are lower for the B type systems, that can be again an evidence of the fast decrease of T_g with the POSS content. This decrease for the two higher POSS contents could be related with a possible effect of thermal degradation of these systems during cure, due to the long time, 7.5 h, that the system was at 120°C.

From second scans (Fig. 5) it can be concluded that T_g decreases with the POSS content and for samples with 10 and 20% of POSS, obtained T_g values for B samples are lower than those corresponding to similar samples cured through the short curing cycle. This could be related again with a possible degradation of the system.

During second DSC scans no residual heat was detected for any sample. This is indicative that the system has completely reacted, at least on the range of temperatures studied. It can be merely mentioned that endothermic peaks were detected at temperatures

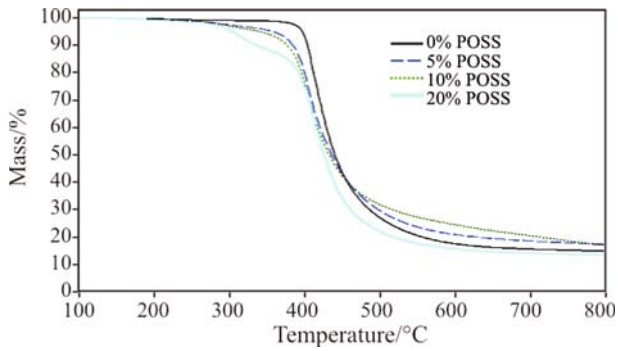

Fig. 6 TG curves corresponding to the samples cured through the short curing cycle (A samples)

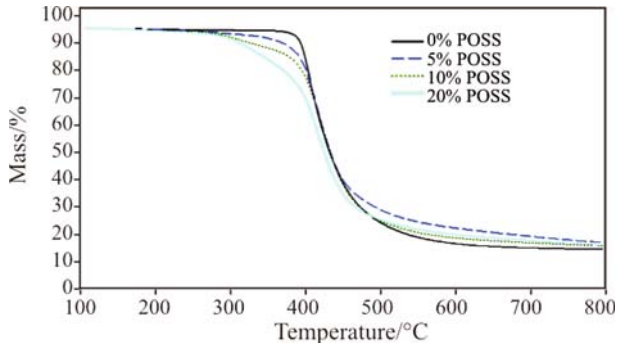

Fig. 7 TG curves corresponding to the samples cured through the long curing cycle (B samples)

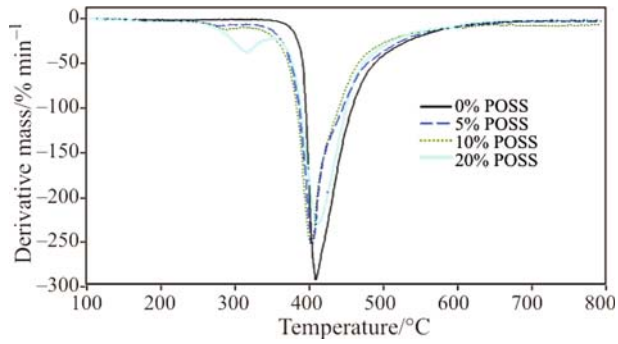

Fig. 8 DTG curves corresponding to the samples cured through the short curing cycle (A samples)

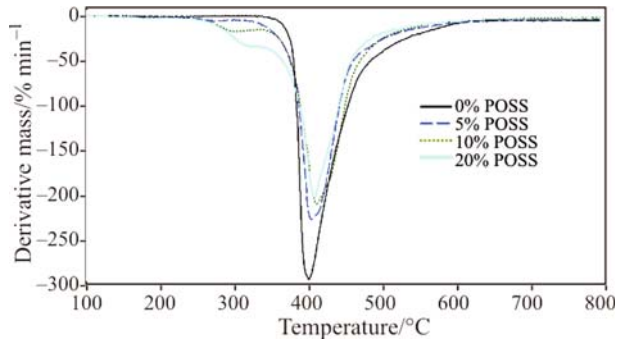

Fig. 9 DTG curves corresponding to the samples cured through the long curing cycle (B samples)

around 160°C. The intensity of these peaks increases with the POSS content and do not appear for samples without POSS, so they possibly are associated to a melting event of the POSS.

According to these results, the 'best' curing cycle should be the 'short' one, although not only the final glass transition temperature is the key to select certain curing cycle. Properties such as elastic modulus, thermal stability, etc. are of great importance and it will be the objective of future works.

Thermogravimetric analysis (TG)

Figures 6 and 7 show thermal degradation curves (TG curves) corresponding to dynamic experiments carried out at the heating rate of 20°C min^{-1}, for A and B systems, respectively.

According to their shape, these curves are two type: [21] for 0% POSS systems, curves are C type, a single-state decomposition reaction where the procedural decomposition temperatures, initial and final, are well defined, but for the samples with POSS, thermodegradation curves are more similar to E type curves, where the individual reaction steps are not very well defined. From Figs 6 and 7 it can be observed that there is a light and slow mass loss before the main decomposition step (due to the thermal degradation of the epoxy resin and at a temperature around 380°C) that can be attributed to the presence of POSS on the samples, because this first decomposition step was not detected for samples without POSS. In the case of type E curves, derivative thermogravimetric curves (DTG curves) are often preferred [21]. Owing to that, derivative curves for the short and long curing cycles are presented in Figs 8 and 9, respectively. In both cases, it can be observed that this first peak on the derivative curve shifts to higher temperatures as the POSS content is increased (also Table 3). It can also be mentioned that shapes of derivative curves are quite different when short and long curing cycles are compared. That can be due to a possible difference between the locations of POSS on the two types of epoxy networks, which maybe have been conditioned for the selected curing sequences.

The relative thermal stability of the different cured systems was evaluated through different parameters. Firstly, the onset and endset temperatures of the thermodegradation process, T_o and T_e, respectively, as well as the width of the reaction interval T_e–T_o, can be obtained from TG curves using the TG software. Crossing points between the baselines (before the mass loss begins and when it has been finished) and the tangent to the curve on the 'main' inflection point were considered. Onset and

Table 1 Onset and endset temperatures and reaction interval for short and long cured systems

% POSS	Short curing cycle			Long curing cycle		
	T_o/°C	T_e/°C	T_e–T_o/°C	T_o/°C	T_e/°C	T_e–T_o/°C
0	397.35	459.15	61.81	388.69	454.86	66.17
5	383.75	451.36	67.61	383.63	454.23	70.60
10	379.33	444.73	65.40	383.61	465.23	81.62
20	378.59	459.77	81.18	372.73	454.25	81.52

endset temperatures values for all the studied systems are shown in Table 1. As it can be seen, there is a slow decrease on the onset temperatures compared with the systems without POSS, but this change is not very significant when considering only values for systems with POSS. As the endset temperatures do not suffer strong changes, there is an increase in the reaction interval obtained as the difference T_e–T_o. In this case, there is a clear dependence on the POSS content. This is obviously due to the first mass loos step suffered for all systems with POSS.

Another common criterion to depict the thermal degradation is the study of the temperature at which there has been a 5% mass loss [22–25]. According to this method, obtained values are shown in Table 2. As the POSS content increases, temperatures at which there has been a 5% mass loss decrease. It can also be observed some differences between the values for the long and short curing cycles corresponding to the same POSS content, but the behavior is not well defined.

The last employed criterion to compare the thermal stability of these systems was evaluating the temperature at which degradation reaction attain a maximum rate, which corresponds to the inflection point temperatures, T_m. These T_m values, determined from the minimum of the DTG curves and residues, R (%), after complete degradation (800°C) are shown in Table 3. As it can be seen, the inflection point temperature corresponding to the first step, T_{m1rst}, strongly depends on the POSS content, but the main decay in the change of mass, T_{m2nd}, is similar for all the compositions.

Analysis of these curves shows that, at 800°C, the residue does not suffers a significant dependence on the POSS content.

Table 2 5% mass loss temperatures for short and long cured systems

% POSS	5% mass loss temperature/°C	
	Short curing cycle	Long curing cycle
0	398.17	390.63
5	359.37	363.28
10	341.97	317.61
20	304.70	306.69

Kinetic study

According to Doyle approximation [14], conversion values between 5 and 35% were used. Best fitting solid state mechanisms and corresponding activation energies and fitting correlations obtained using the three mentioned methods are shown in Table 4. This table suggests that both, reaction solid state mechanism of thermal degradation and activation energy are not affected for the curing cycle selection. For samples without POSS, the mechanism that better fits to the experimental data is a deceleratory mode, F_2 or F_3. Selecting mode F_3, as this is the only that fits well in the three employed methods, the activation energy of the reaction of thermal degradation is around 114 kJ mol^{-1}. For samples containing different concentrations of POSS, the mechanism is D_1 or R_1, being the corresponding energies dependent on the POSS content. In most cases, whatever mechanism is predominant, activation energies are higher than those corresponding to the same system without POSS. Although, as the percentage of POSS is increasing, activation energies decrease, reaching even in some

Table 3 Inflection point temperatures and residues at 800°C for short and long curing cycles

% POSS	Short curing cycle			Long curing cycle		
	T_{m1rst}/°C	T_{m2nd}/°C	R/%	T_{m1rst}/°C	T_{m2nd}/°C	R/%
0	–	410.59	15.16	–	404.49	15.45
5	279.31	405.80	17.55	274.45	407.89	17.96
10	289.55	404.67	17.33	308.25	414.38	16.72
20	317.67	413.22	13.65	325.28	413.07	16.83

Table 4 Best fitting models, activation energies (kJ mol^{-1}) and correlations obtained using Coats-Redfern, Horowitz- Metzger and Van Krevelen methods for the different concentrations of POSS, corresponding to the short and long curing cycles

Curing cycle	% Poss	Coats-Redfern			Horowitz-Metzger			Van Krevelen		
		Mode	E_a/kJ mol^{-1}	R	Mode	E_a/kJ mol^{-1}	R	Mode	E_a/kJ mol^{-1}	R
Short	0	F3	109.15	0.99954	F3	119.89	0.99969	F3	114.40	0.99963
					F2	59.94	0.99969	F2	54.36	0.99963
	5	R1	164.37	0.99920	R1	180.19	0.99954	R1	172.20	0.99942
		D1	339.88	0.99924	D1	360.39	0.99954	D1	350.05	0.99942
		D2	351.43	0.99907	D2	372.27	0.99942	D2	361.76	0.99928
		D4	355.46	0.99901	D4	376.41	0.99937	D4	365.85	0.99922
	10	R1	137.01	0.99787	R1	153.83	0.99857	R1	145.30	0.99830
		D1	285.08	0.99771	D1	307.66	0.99857	D1	296.23	0.99830
		D2	294.79	0.99758	D2	317.77	0.99833	D2	306.14	0.99805
		D4	298.19	0.99748	D4	321.29	0.99825	D4	309.59	0.99796
	20	R1	101.93	0.99924	R1	116.80	0.99960	R1	118.03	0.99950
		D1	215.10	0.99931	D1	233.61	0.99960	D1	241.78	0.99950
		D2	227.50	0.99912	D2	246.43	0.99947	D2	236.86	0.99934
		D4	231.96	0.99904	D4	251.03	0.99942	D4	241.39	0.99928
Long	0	F3	106.436	0.99922	F3	118.11	0.99952	F3	112.26	0.99944
		F2	47.59	0.99904	F2	59.05	0.99952	F2	53.32	0.99944
	5	R1	160.13	0.99938	R1	175.48	0.99964	R1	167.73	0.99955
		D1	331.44	0.99942	D1	350.97	0.99964	D1	341.12	0.99955
		D2	342.73	0.99929	D2	362.55	0.99956	D2	352.56	0.99945
		D4	346.67	0.99924	D4	366.59	0.99952	D4	356.55	0.99942
	10	R1	90.42	0.99309	R1	108.42	0.9958	R1	99.20	0.99513
		D1	191.90	0.99381	D1	216.85	0.9958	D1	204.10	0.99513
		D2	198.52	0.99331	D2	223.93	0.99494	D2	210.95	0.99469
		D4	200.83	0.99313	D4	226.40	0.99524	D4	213.34	0.99453
	20	R1	68.11	0.99542	R1	83.42	0.99743	R1	75.60	0.99701
		D1	147.33	0.99604	D1	116.83	0.99743	D1	156.90	0.99701
		D2	155.97	0.99557	D2	175.94	0.99705	D2	165.77	0.99659
		D4	159.07	0.99539	D4	179.21	0.9969	D4	168.95	0.99643

cases, lower values than that of the same system without POSS. Anywhere, it can be said that the addition of POSS changes the reaction solid state mechanism of the thermodegradation reaction, from a F_n to a D_n or R_n mechanisms.

Conclusions

The thermal degradation of the epoxy system DGEBA (*n*=0)/mXDA with different amounts of polyhedral oligomeric silsesquioxanes (POSS) nanoparticles was studied by TG in order to determine the influence of both, the POSS concentration and the curing cycle on the reaction mechanisms of the decomposition process. No improvement on the thermal stability was detected with the addition of POSS but neither significant worsening was observed.

Various integral methods were used for the kinetic study of the thermal degradation process. The interpretation of results obtained through these integral methods, allows confirmation that the system follows different thermodegradation mechanism depending if the system contains or not POSS nanoparticles. Al-

though no differences on the thermodegradation mechanism were observed between systems containing various amounts of POSS, activation energies show a clear dependence with the POSS content; as the concentration of nanoparticles is increasing, the activation energy decreases.

Glass transition temperatures were determined by DSC and different behaviors were observed according to the curing cycle selected. Samples cured through the short cycle showed rising T_g values as the percentage or POSS increases until 10%, but T_g of samples cured through the long cycle decreased with the POSS content. No residual heat was detected for any sample thus concluding that the system has completely reacted, at least on the range of temperatures studied. Endothermic peaks were detected at temperatures around 160°C. These peaks were related to a melting event of the POSS present in the samples.

References

1 C. U. Pittman Jr., G.-Z. Li and H. Ni, Macromol. Symp., 196 (2003) 301.
2 F. Fraga, T. Salgado, J. A. Rodríguez Añón and L. Núñez Regueira, J. Thermal. Anal., 41 (1994) 1543.
3 R. A. Mantz, P. F. Johns, K. P. Chaffee, J. D. Lichtenhan and J. W. Gilman, Chem. Mater., 8 (1996) 1250.
4 A. Sellinger and R. M. Laine, Macromolecules, 29 (1996) 2327.
5 T. S. Haddad and J. D. Lichtenhan, Macromolecules, 29 (1996) 7302.
6 R. M. Laine, C. Zhang, A. Sellinger and L. Viculis, Appl. Organomet. Chem., 12 (1988) 707.
7 E. G. Shockey, A. G. Bolf, P. F. Jones, J. J. Schwab, K. P. Chaffee, T. S. Haddad and J. D. Lichtenhan, Appl. Organomet. Chem., 13 (1999) 311.
8 J. J. Schwab, T. S. Haddad, J. D. Lichtenhan, P. T. Mather and K. P. Chaffee, Proceedings of the Society of Plastics Engineers, 54th ANTEC; 1997; Vol. 611, 1817.
9 Carmen Ramírez, M. Rico, L. Barral, J. Díez, S. García-Garabal and B. Montero, J. Therm. Anal. Cal., 87 (2007) 69.
10 F. Román, S. Montserrat and J. M. Hutchinson, J. Therm. Anal. Cal., 87 (2007) 113.
11 L. Núñez, F. Fraga, L. Fraga and J. A. Rodríguez, J. Thermal Anal., 47 (1996) 743.
12 B. Ellis, Chemistry and Technology of Epoxy Resins, Blackie Academic and Professional, 1st Ed., U. K. 1993.
13 L. Núñez, F. Fraga, M. R. Núñez and M. Villanueva, Polymer, 41 (2000) 4635.
14 C. D. Doyle, Nature, 207 (1965) 240.
15 H. E. Kissinger, Anal. Chem., 29 (1957) 1702.
16 J. H. Flynn and L. A. Wall, J. Res. Nat. Bur. Standards A Phys. Chem., 70 A (1996) 487.
17 A. W. Coats and J. P. Redfern, Nature, 207 (1965) 290.
18 H. Lee and K. Neville, Handbook of Epoxy Resin, McGraw-Hill, New York 1967.
19 L. Núñez, J. Taboada, F. Fraga and M. R. Núñez, J. Appl. Polym. Sci., 66 (1997) 1377.
20 Lisardo Núñez, L. Fraga, M. R. Núñez, M. Villanueva and B. Rial, J. Therm. Anal. Cal., 70 (2002) 9.
21 T. Hatakeyama and F. X. Quinn, Thermal Analysis, Fundamentals and Applications to Polymer Science, Wiley, England 1994.
22 De Chirico, M. Armanini, P. Chini, G. Cioccolo, F. Provasoli and G. Audisio, Polym. Degrad. Stab., 79 (2003) 139.
23 H. S. Kim, H. S. Yang and H. J. Park, J. Therm. Anal. Cal., 76 (2004) 395
24 B. Xiao, X. F. Sun and R. C. Sun, Polym. Degrad. Stab., 71 (2001) 223
25 N. Nishioka, M. Yamaoka, H. Haneda, K. Kawakami and M. Uno, Macromolecules, 26 (1993) 4694.

Received: May 6, 2008
Accepted: August 12, 2008
Online First: January 12, 2009

DOI: 10.1007/s10973-008-9213-x